Anal. Chem. **2002,** *74,* 5076−5083

Microfabricated 384-Lane Capillary Array Electrophoresis Bioanalyzer for Ultrahigh-Throughput Genetic Analysis

Charles A. Emrich,[†] Huijun Tian,[‡,§] Igor L. Medintz,[‡,||] and Richard A. Mathies*[,‡]

Department of Chemistry and Biophysics Graduate Group, University of California, Berkeley, California 94720

A microfabricated 384-lane capillary array electrophoresis device is developed and utilized for massively parallel genetic analysis. The 384 capillary lanes, arrayed radially about the center of a 200-mm-diameter glass substrate sandwich, are constructed using scalable microfabrication techniques derived from the semiconductor industry. Samples are loaded into reservoirs on the perimeter of the wafer, separated on the 8-cm-long poly(dimethylacrylamide) gel-filled channels, and detected with a four-color rotary confocal fluorescence scanner. The performance and throughput of this bioanalyzer are demonstrated by simultaneous genotyping 384 individuals for the common hemochromatosis-linked H63D mutation in the human *HFE* gene in only 325 s. This lab-on-a-chip device thoroughly exploits the power of microfabrication to produce high-density capillary electrophoresis arrays and to use them for high-throughput bioanalysis.

Advanced instrumentation is enhancing our understanding of genetic variation, diagnostic mutations, functional genomics, and pharmacogenomic tailoring of clinical treatments. For example, the introduction of capillary array electrophoresis (CAE)[1−3] was a breakthrough in the Human Genome Project that significantly accelerated progress. Since then, CAE systems have been the workhorse for sequencing dozens of organisms and have become the gold standard for the analysis of genetic variation. Despite this success, enhancing the speed and parallelism of electrophoretic analysis is a critical goal. Microfabricated CAE (μCAE) devices are now poised to provide this next generation of genetic analysis systems owing to their improved performance, design flexibility, ease of fabrication, and potential for low-volume, on-chip integration of sample preparation.

The first microfabricated separation systems[4] emphasized the ability of miniaturization to increase performance by reducing analysis times and reagent volumes. Capillary electrophoresis (CE) channels microfabricated on glass chips were then used to perform separations of fluorescent dyes[5,6] and amino acids.[7] DNA separations were first demonstrated by Woolley and Mathies on a single-lane device,[8] and subsequent work has significantly increased the lane density.[9−12] The highest throughput and performance so far was enabled by the transition to radial capillary arrays detected using a rotary confocal fluorescence scanner.[13,14] Building on the success of this new format, we were interested in producing μCAE fluidic networks that push the limits of channel density and using them for high-throughput evaluation of genetic variation.

Hereditary hemochromatosis (HHC) is an excellent model system for evaluating the utility of high-density CAE microdevices. HHC is one of the most common autosomal recessive diseases in the United States,[15] characterized by increased iron absorption by intestinal epithelial cells,[16] eventually resulting in iron overload manifest by cirrhosis, cardiomyopathy, diabetes mellitus, and other complications. Phlebotomy can be used as an effective and

* Corresponding author. Phone: (510) 642-4192, Fax: (510) 642-3599. E-mail: rich@zinc.cchem.berkeley.edu.

[†] Biophysics Graduate Group.

[‡] Department of Chemistry.

[§] Current address: Department of Biochemistry and Molecular Biology, Indiana University, Indianapolis, IN 46202.

[||] Current address: Center for Bio/Molecular Science and Engineering, U.S. Naval Research Laboratory, Washington, DC 20375.

(1) Mathies, R. A.; Huang, X. C. *Nature* **1992**, *359*, 167−169.

(2) Kambara, H.; Takahashi, S. *Nature* **1993**, *361*, 565−566.

(3) Zhang, J.; Voss, K. O.; Shaw, D. F.; Roos, K. P.; Lewis, D. F.; Yan, J.; Jiang, R.; Ren, H.; Hou, J. Y.; Fang, Y.; Puyang, X.; Ahmadzadeh, H.; Dovichi, N. J. *Nucleic Acids Res.* **1999**, *27*, e36.

(4) Manz, A.; Miyahara, Y.; Miura, J.; Watanabe, Y.; Miyagi, H.; Sato, K. *Sens. Actuators* **1990**, *B1*, 249−255.

(5) Harrison, D. J.; Fluri, K.; Seiler, K.; Fan, Z. H.; Effenhauser, C. S.; Manz, A. *Science* **1993**, *261*, 895−897.

(6) Manz, A.; Harrison, D. J.; Verpoorte, E. M. J.; Fettinger, J. C.; Paulus, A.; Ludi, H.; Widmer, H. M. *J. Chromatogr.* **1992**, *593*, 253−258.

(7) Jacobson, S. C.; Hergenroder, R.; Moore, A. W.; Ramsey, J. M. *Anal. Chem.* **1994**, *66*, 4127−4132.

(8) Woolley, A. T.; Mathies, R. A. *Proc. Natl. Acad. Sci. U.S.A.* **1994**, *91*, 11348−11352.

(9) Simpson, P. C.; Roach, D.; Woolley, A. T.; Thorsen, T.; Johnston, R.; Sensabaugh, G. F.; Mathies, R. A. *Proc. Natl. Acad. Sci. U.S.A.* **1998**, *95*, 2256−2261.

(10) Huang, Z.; Munro, N.; Huhmer, A. F. R.; Landers, J. P. *Anal. Chem.* **1999**, *71*, 5309−5314.

(11) Liu, S. R.; Ren, H. J.; Gao, Q. F.; Roach, D. J.; Loder, R. T.; Armstrong, T. M.; Mao, Q. L.; Blaga, I.; Barker, D. L.; Jovanovich, S. B. *Proc. Natl. Acad. Sci. U.S.A.* **2000**, *97*, 5369−5374.

(12) Backhouse, C.; Caamano, M.; Oaks, F.; Nordman, E.; Carrillo, A.; Johnson, B.; Bay, S. *Electrophoresis* **2000**, *21*, 150−156.

(13) Shi, Y.; Simpson, P. C.; Scherer, J. R.; Wexler, D.; Skibola, C.; Smith, M. T.; Mathies, R. A. *Anal. Chem.* **1999**, *71*, 5354−5361.

(14) Medintz, I.; Wong, W. W.; Berti, L.; Shiow, L.; Tom, J.; Scherer, J.; Sensabaugh, G.; Mathies, R. A. *Genome Res.* **2001**, *11*, 413−421.

(15) Steinberg, K. K.; Cogswell, M. E.; Chang, J. C.; Caudill, S. P.; McQuillan, G. M.; Bowman, B. A.; Grummer-Strawn, L. M.; Sampson, E. J.; Khoury, M. J.; Gallagher, M. L. *JAMA, J. Am. Med. Assoc.* **2001**, *285*, 2216−2222.

(16) Zoller, H.; Pietrangelo, A.; Vogel, W.; Weiss, G. *Lancet* **1999**, *353*, 2120−2123.

10.1021/ac020236g CCC: $22.00
Published on Web 08/27/2002

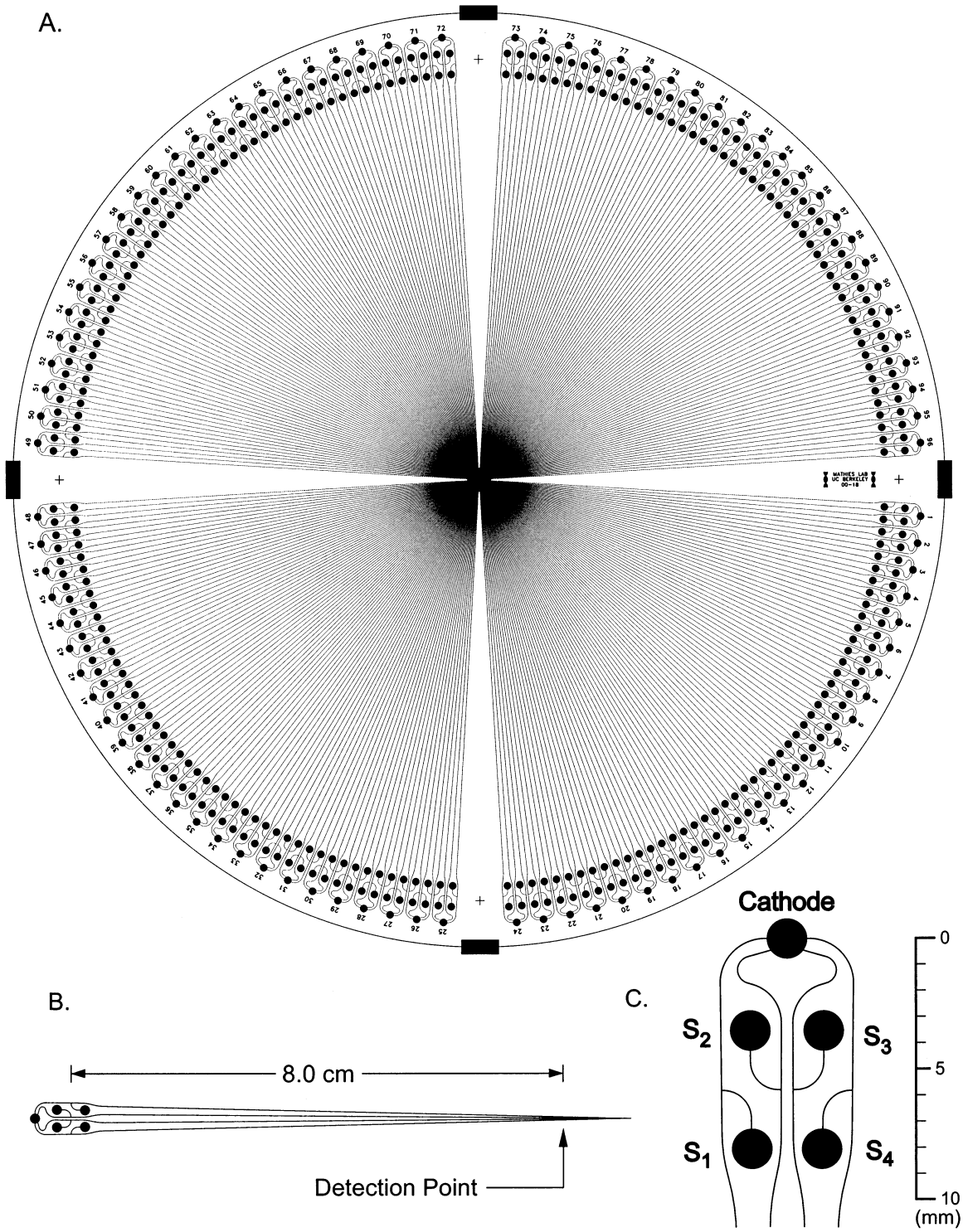

Figure 1. (A) Layout of the 384-lane μCAE device on a 200-mm -diameter wafer. Lanes are ~60 μm wide and 30 μm deep, and the effective separation length is 8.0 cm. (B) Expanded view of a single quartet of channels with their injectors. (C) All channels in a quartet share a common cathode reservoir located closest to the edge of the wafer. The injector design for every channel is shown at right. S_1 − S_4 indicate individual sample reservoirs.

successful treatment,[17] but diagnosis of the disease remains an obstacle, as the traditional transferrin saturation/serum ferritin assays can be inconclusive due to variation in phenotypic severity.[18] Additionally, confirmation of the disease phenotype requires clinical visits and often a liver biopsy, all of which could be mitigated by conclusive genetic screening.

The *HFE* gene has been linked to HHC occurrence through at least two missense SNP mutations, C282Y and H63D.[19] Individuals homozygous for the less common C282Y mutation show a 50−100% penetrance, while compound C282Y/H63D

(17) Niederau, C.; Fischer, R.; Purschel, A.; Stremmel, W.; Haussinger, D.; Strohmeyer, G. *Gastroenterology* **1996**, *110*, 1107−1119.

heterozygotes and H63D homozygotes are also at elevated risk for hemochromatosis. Although population-based screening has not yet been recommended,[20] the large numbers of assays necessary for this consensus statement and supporting studies[15,21] demonstrate the need for reliable high-throughput genetic testing.

To address these needs, we have developed a 384-lane μCAE device capable of performing multiplexed electrophoretic DNA analyses many times faster than conventional methodology. After PCR amplification and 63H-specific enzymatic digestion, samples from 384 individuals are electrophoretically analyzed on the microdevice in 7 min and genotyped with 98.7% accuracy. This performance was realized by high-fidelity fabrication of a high-density array of microcapillaries with supporting injectors on 200-mm-diameter glass wafers. This is the highest throughput genotyping achieved with any electrophoretic system, outperforming conventional 96-capillary instrumentation by over 20-fold.

MATERIALS AND METHODS

Microchip Preparation and Design. Borosilicate glass wafers (Borofloat, Schott, Yonkers, NY) were cleaned and coated with 2000 Å of silicon by dc magnetron sputtering. Photoresist (Shipley 1818, Marlborough, MA) was spun onto the wafer, and the channel pattern was transferred by UV exposure in a contact printer (Illumination Industries, Sunnyvale, CA). After developing, the exposed Si hard mask was reactive ion etched in a SF_6 plasma (PlasmaTherm, St. Petersburg, FL). Channels were then wet etched into the wafer with concentrated HF. Isotropic etching of the channels to a depth of 30 μm required 4 min. Reservoirs were drilled with 1.5-mm-diameter diamond bits on a CNC mill. The remaining silicon was then removed by plasma etching. The wafer and a blank wafer of the same size (200-mm diameter, 1.1 mm thick) were cleaned, placed face to face, and bonded together at 680 °C by thermal compression sintering. Channels in the μCAE device were coated to prevent DNA adsorption and electroosmotic flow using a modified version of the Hjertén protocol.[22]

The layout of the 384-lane μCAE chip is presented in Figure 1. Four quadrants of 24 quartets are distributed radially about the central anode reservoir. A quartet consists of an apical, common cathode reservoir and four sample reservoirs connected to their respective separation lanes by a T-injector (Figure 1B). A blowup of the injector region (Figure 1C) shows the coat hanger shape in the inner two channels, which equalizes the lengths of all four channels for uniform pressure-driven loading of the sieving matrix from the central anode. This structure also provides uniform injection plug sizes and electrophoresis times in all lanes. The 200-mm-diameter substrate accommodates a minimal distance of 1.2 mm between each of the 1.5-mm-diameter sample reservoirs. We have eliminated the fourth "waste" reservoir usually employed in microchip CE systems[23] in favor of a direct injection format. This design considerably reduces the area of each quartet at the expense of a less well-defined injection plug because the smaller, higher mobility DNA fragments are preferentially loaded. This size-biased injection effect is minimized by injecting for a short time and by using a multiple-step electrokinetic injection method (see below).

Sample Preparation. The DNA samples were drawn from the Centre d'Etude du Polymorphisme Humain (CEPH) panel of 100 reference Caucasian samples (HD100CAU), CEPH family 00884 as well as CEPH samples NA10859 (universal CEPH donor sample), NA14620, NA14641, and NA14690 (Coriell Cell Repositories, Camden, NJ). Additional samples were drawn from a Swiss and an Austrian population, both generously provided by G. Sensabaugh (U. C. Berkeley School of Public Health).

PCR reactions utilized Qiagen (Valencia, CA) PCR Master Mix with 50 ng of genomic DNA and 15 pmol of primer added to each 25-μL reaction volume. Two sets of PCR primers were utilized for amplification: H63D-1 5′-gcctcaacatcctgctcccctcc-3′, H63D-2 5′-tcccctcctactacacat ggttaaggcc-3′, H63D-3 5′-tcccctccta ctacacatgg-3′, and H63D-4 5′-tcagctgcagccacatctggc-3′.[14,18] Use of primers H63D-1 and H63D-4 yields a 246-bp product while H63D-2/3 and H63D-4 yield a 231-bp product. Following a step-down thermal cycling profile,[23] successful PCR amplification was verified on agarose gels prior to restriction digestion.

The presence of the H63D (187c→g) substitution in each amplicon was determined by digestion with *Mbo*I (Gibco BRL, Gaithersburg, MD). The wild-type amplicon undergoes digestion at the 5′-end of the 5′-gatc recognition site while the variant amplicon remains undigested. The 246-bp amplicon yielded fragments of 172 and 74 bp while the 231-bp amplicon yielded digested fragments of 157 and 74 bp. Digested samples were desalted by spin dialysis (Microcon YM-10, Millipore, Bedford, MA), resuspended in 10 mM Tris-EDTA (TE), and then mixed 1:7 with a 1:30 dilution of a 100-bp ladder (GeneChoice DNA Ladder II, PGC Scientifics, Frederick, MD) also in 10 mM TE.

Separation and Detection. The 5% v/v poly(*N*,*N*-dimethylacrylamide) (PDMA) short-chain sieving matrix was prepared by solution-phase polymerization of *N*,*N*-dimethylacrylamide (Aldrich, Milwaukee, WI) with 0.004% w/v ammonium persulfate (Sigma, St. Louis, MO), 0.1% v/v *N*,*N*,*N*′,*N*′-tetramethylethylenediamine (Bio-Rad Laboratories, Hercules, CA), 1% v/v 2-propanol, and 1× TBE under helium for 20 h.[24] The sieving matrix was mixed with 1 μM thiazole orange for fluorescent labeling of DNA fragments.

Channels were filled with the PDMA sieving matrix within 1 min by pumping gel at 100 psi through the central anode reservoir using a high-pressure loader.[25] Genotyping samples and 1× TBE buffer were added to individual wells on the μCAE chip using a single-probe Hamilton MicroLab 4000 (Hamilton, Reno, NV). Loading 3.0 μL of sample to each of the 384 sample reservoirs and 3.0 μL to each of the 96 common cathode reservoirs required 42 min. A multiple-probe instrument has been separately developed that reduces this time to 5 min (Ezra van Gelder, personal communication).

(18) Mura, C.; Nousbaum, J. B.; Verger, P.; Moalic, M. T.; Raguenes, O.; Mercier, A. Y.; Ferec, C. *Hum. Genet.* **1997**, *101*, 271−276.

(19) Feder, J. N.; Gnirke, A.; Thomas, W.; Tsuchihashi, Z.; Ruddy, D. A.; Basava, A.; Dormishian, F.; Domingo, R.; Ellis, M. C.; Fullan, A.; Hinton, L. M.; Jones, N. L.; Kimmel, B. E. *Nat. Genet.* **1996**, *13*, 399−408.

(20) Burke, W.; Thomson, E.; Khoury, M. J.; McDonnell, S. M.; Press, N.; Adams, P. C.; Barton, J. C.; Beutler, E.; Brittenham, G.; Buchanan, A.; Clayton, E. W.; Cogswell, M. E.; Meslin, E. M. *JAMA, J. Am. Med. Assoc.* **1998**, *280*, 172−178.

(21) Beutler, E.; Felitti, V.; Gelbart, T.; Ho, N. *Ann. Intern. Med.* **2000**, *133*, 329−337.

(22) Hjerten, S. *J. Chromatogr.* **1985**, *347*, 191−198.

(23) Medintz, I.; Wong, W. W.; Sensabaugh, G.; Mathies, R. A. *Electrophoresis* **2000**, *21*, 2352−2358.

(24) Heller, C. *Electrophoresis* **1999**, *20*, 1978−1986.

(25) Scherer, J. R.; Paegel, B. M.; Wedemayer, G. J.; Emrich, C. A.; Lo, J.; Medintz, I. L.; Mathies, R. A. *Biotechniques* **2001**, *31*, 1150-1153.

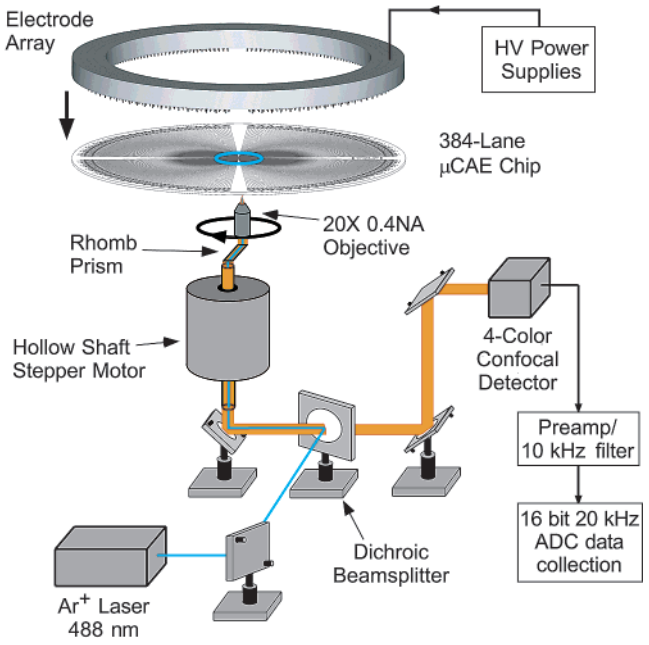

Figure 2. The Berkeley rotary confocal fluorescence scanner used to detect μCAE chip separations. Laser excitation at 488 nm (100 mW) is directed up through the hollow shaft of a computer-controlled stepper motor, deflected 1.0 cm off-axis by a rhomb prism, and focused on the electrophoresis lanes by a 20× 0.4 NA microscope objective. The stepper motor rotates the rhomb/objective assembly just under the lower surface of the μCAE microchip at 5 revolutions/s. Fluorescence is collected along the same path and spectrally and spatially filtered before impinging on the detector (30-nm band-pass at 520 nm).

The Berkeley rotary confocal fluorescence scanner[13] can be used to detect a wide variety of chip formats ranging from 96 channels on a 100-mm substrate to the current 384 on a 200-mm substrate. The scanner, depicted in Figure 2, utilizes the 488-nm beam from an Ar^+ laser directed up through the hollow shaft of a computer-controlled stepper motor, deflected 1 cm from the axis of rotation by a rhomb prism, and then directed through a microscope objective (20×, 0.4 NA), which rotates at 5 Hz just under the lower surface of the chip. Fluorescence is collected through the same path and passed to a four-color confocal PMT detector.

The μCAE chip is positioned on the temperature-controlled stage (30 °C) and an electrode array ring put in place, dipping each electrode into its corresponding reservoir. The 384 lane locations were defined by measuring the Raman scattering of water in the third (580 nm) channel of the PMT detector array. Electrokinetic injection was accomplished by applying +200, +2000, and 0 V, respectively, to the cathode, anode, and sample reservoirs for 25 s with high-voltage power supplies. During this phase, the analyte is electrokinetically driven from the sample reservoir toward both the cathode and anode reservoirs. Initial electrophoresis was carried out with the anode at 2000 V, the cathode at 0 V, and the sample floating. After 25 s, the anode potential was increased to +2500 V, and a +400 V back-biasing potential was applied to the sample reservoir to prevent leakage of DNA onto the separation column. This delayed back-biasing was necessary to allow sufficient loading of higher molecular weight DNA fragments. Fluorescence is collected at 520, 550, 580, and 605 nm by PMTs, electronically filtered at 10 kHz, and digitized by a 16-bit, 24-kHz ADC allowing 13-μm resolution along the path of rotation.

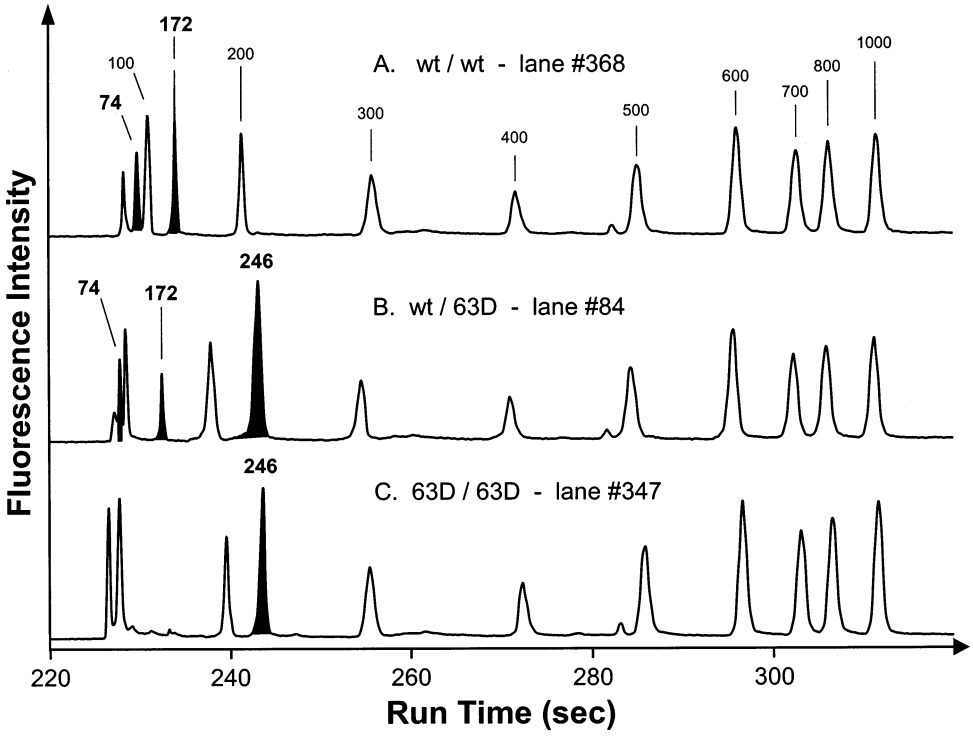

Figure 3. Representative electropherograms from a 384-lane μCAE run illustrating each of the three possible genotypes: (A) homozygous wild type, (B) heterozygous, and (C) homozygous for the H63D missense mutation. The highlighted PCR−RFLP fragment peaks are found at 246 (63D mutant) and 172 bp (wild type). Samples are co-injected with a 100-bp size standard. Thiazole orange was added to the 5% v/v PDMA sieving matrix for fluorescent labeling. Electrophoresis was carried out at 260 V/cm.

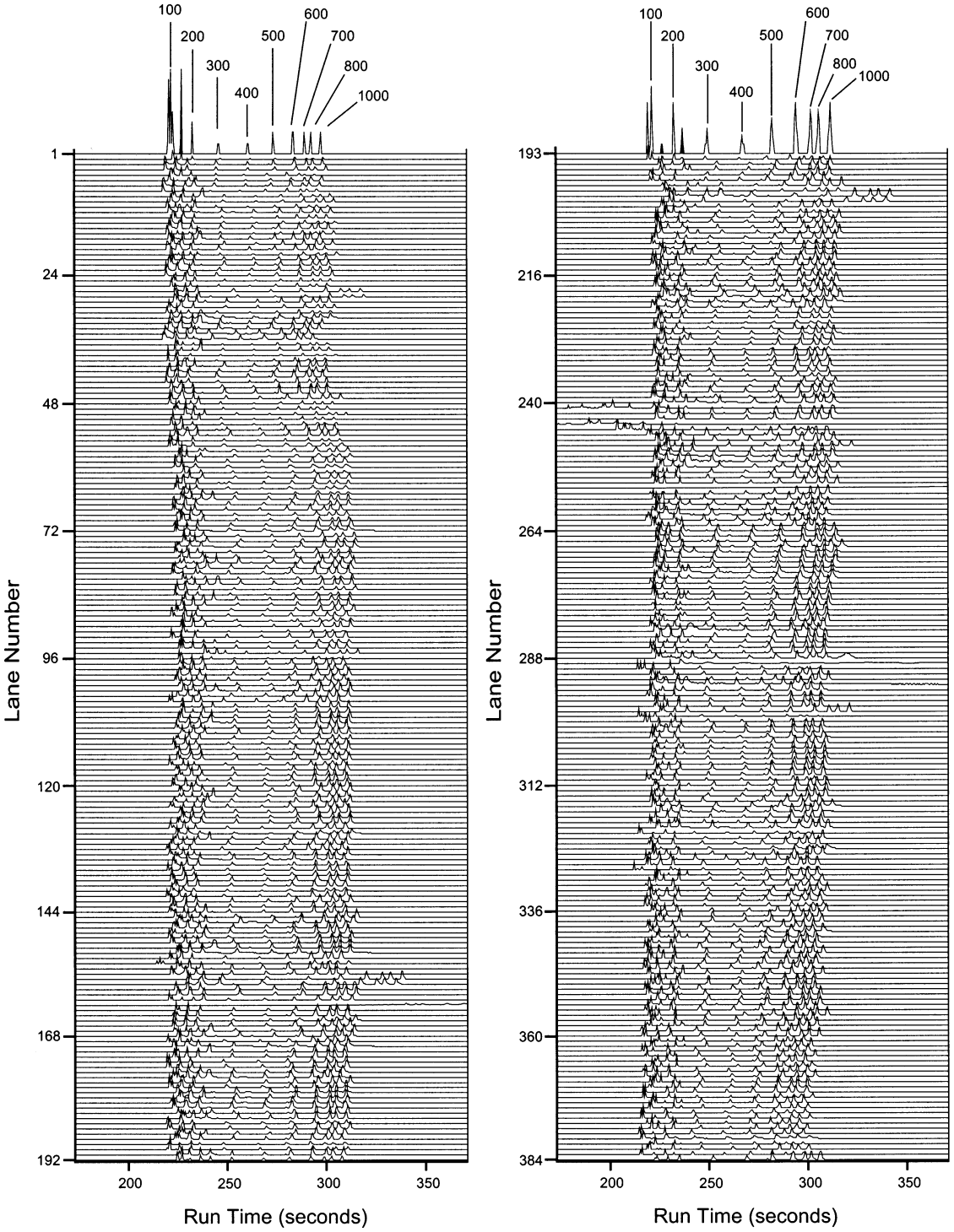

Figure 4. Electropherograms from a HHC genotyping run on the 384-lane μCAE chip. RFLP fragments are highlighted in black in lanes 1 (wild type) and 193 (heterozygote). Genotyping of the samples was possible in 379 lanes (98.7% success rate). Electrophoresis was complete within 325 s.

RESULTS AND DISCUSSION

To evaluate the 384-lane μCAE device performance, we performed PCR−RFLP-based genotyping of 384 individuals for the H63D missense SNP in *HFE*. The H63D (187c→g) mutation was detected by digestion of a PCR product with *Mbo*I. Mutant amplicons (246 bp) remain undigested while wild-type amplicons are cleaved into 172- and 74-bp fragments. A single-probe robotic pipettor was used to load 3-μL volumes of sample and electrophoresis buffer into the sample and cathode reservoirs. Electrical addressing of the wells was provided by a modified version of an electrode array ring previously presented[13] that also acted as an enclosure to prevent evaporation of the small fluid volumes (details in supplement: http://www.cchem.berkeley.edu/ramgrp/elsup).

Electrokinetic injection of sample was performed using a delayed back-biasing protocol. The sample is first simultaneously injected toward both the cathode and anode for 25 s. The DNA

plug formed in the separation column has smaller fragments over-represented at the extremities while the larger fragments only reach the T-intersection. After switching to the run configuration, these larger fragments are electrophoresed down the column while the sample reservoir is briefly floated and then switched to a back-biasing potential. The delayed back-biasing prevents sample leakage while removing the small fragment tail as it passes the T-intersection, improving resolution and equalizing injected masses for large and small fragments. Electrophoresis was performed at an electric field of 260 V/cm and was complete within 325 s. The separation was detected with our four-color rotary confocal fluorescence scanner (Figure 2).

Examples of electropherograms from a full 384-lane run showing each genotype are presented in Figure 3. A trace from an individual homozygous for the wild-type allele is shown in Figure 3A. The 172-bp peak is distinct and isolated, while the 74-bp peak is, in this case, resolved from both the ionic front and the 100-bp peaks. Even when the 74- and 100-bp bands are unresolved, the presence of the 172-bp band provides a positive indicator of the wild-type 63H allele. A heterozygous individual exhibits well-resolved peaks at both 172 and 246 bp as shown in Figure 3B. A trace from an individual homozygous for the mutant 63D allele is presented in Figure 3C, showing a strong peak from the undigested 246-bp amplicon. False positive peaks resulting from incomplete digestion of the 246-bp amplicon were observed infrequently (<5% of the lanes) and did not confuse genotyping as they were always less than 10% of the intensity of the positive, digested bands.

Figure 4 presents unprocessed results from a full 384-lane run of the μCAE chip. The peaks from 100 to 1000 bp can be resolved in nearly every lane (379 of 384). Additionally, lane-to-lane variation of the device is extremely low as evidenced by the uniformity of peak positions and heights. The global relative mobility deviation was less than 2.2% for all the lanes and approaches 1.0% for local 20-lane windows. Signal intensity is relatively constant, but greater in the higher numbered channels. This is likely due to evaporative concentration of samples loaded earlier in the process. Examples of electropherograms from successful and from poor or failed lanes are presented in expanded form for evaluation in Figure 5. The poor lanes included those with a mobility deviation of more than 10% or visibly tailed peaks. Peak tailing is most often the result of imperfections during the photolithographic stage of the microfabrication process. The five failed lanes exhibited no peaks or a peak pattern that did not correspond to the ladder. Failures may be due to physical damage to the lane during microfabrication, bubble formation in the channel, or incomplete loading of the PDMA sieving matrix because of channel blockage. Nevertheless, all of the poor lanes can still easily be genotyped, giving a cumulative success rate of 98.7% for the chip. Of the 379 good lanes, 98 were heterozygous and 8 homozygous for the 63D mutant allele, while 273 samples were homozygous for the wild-type 63H allele. The allelic frequency of 15.0% for the mutant D allele was in good agreement with previously published results.[15,21,26]

Our radial 384-lane μCAE device was designed with the goal of providing the maximum number of capillary lanes with a sufficient length for high-resolution separations of dsDNA while working with a compact, easily fabricated wafer. This has been achieved by using a direct injection format with an optimized channel design and PDMA as the sieving matrix. Previous radial microchip CAE devices have been fabricated on 100- and 150-mm-diameter glass wafers, limiting the straight separation channel length to 3.3 and 5.5 cm, respectively. Increasing the wafer diameter to 200 mm permitted 8.0-cm-long lanes, which provide good resolution with the direct injection format. The only drawback is that the direct injection format gives rise to ionic fronts visible as the first peak in all separations. While low molecular weight fragments (<100 bp) may be difficult to visualize, these assays are easily tailored to place all relevant bands above 100 bp.

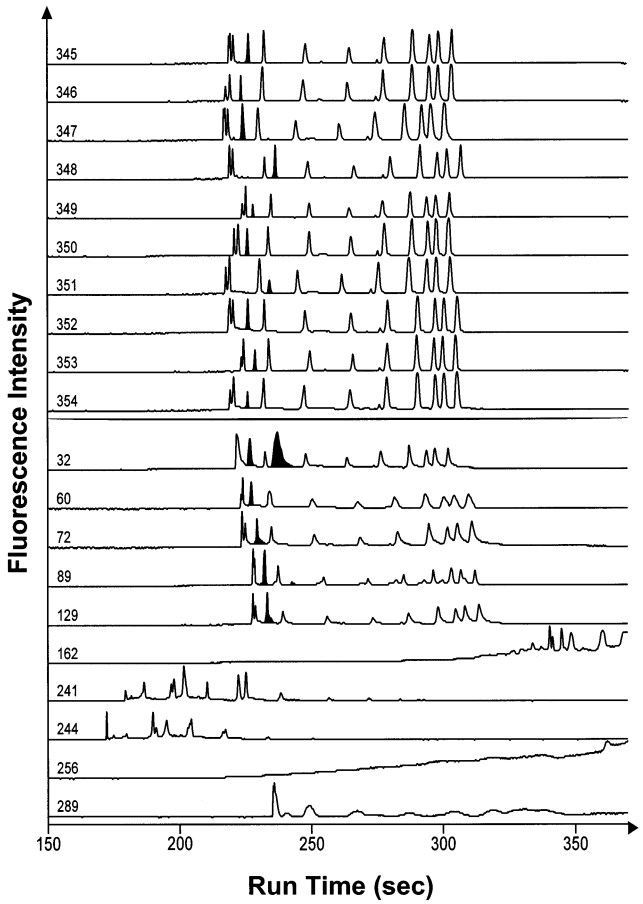

Figure 5. Representative electropherograms presenting good (upper) and poor (lower) lanes from the run in Figure 4. The 10 poor lanes at the bottom include 5 (of 9, from the entire run) that exhibited significant peak tailing or mobility deviations and the 5 lanes that failed outright. Lane numbers are indicated at left.

The multistep direct injection scheme together with the long effective separation length produces better than 10-bp resolution by creating a narrower and more size-inclusive plug than would be achieved using a simple direct injection. Separations of a *Hae*III digest of ϕX174 (data not shown) under similar conditions yielded mean theoretical plate numbers of 4.0×10^6, which compare well to a conventional 30-cm-long capillary. The 271/281-bp ϕX174 peaks were typically baseline resolved, as were all peaks up to 1353 bp.

The direct injector design with delayed back-biasing is a valuable alternative when packing, layout, or other constraints

(26) Whitfield, J. B.; Cullen, L. M.; Jazwinska, E. C.; Powell, L. W.; Heath, A. C.; Zhu, G.; Duffy, D. L.; Martin, N. G. *Am. J. Hum. Genet.* **2000**, *66*, 1246−1258.

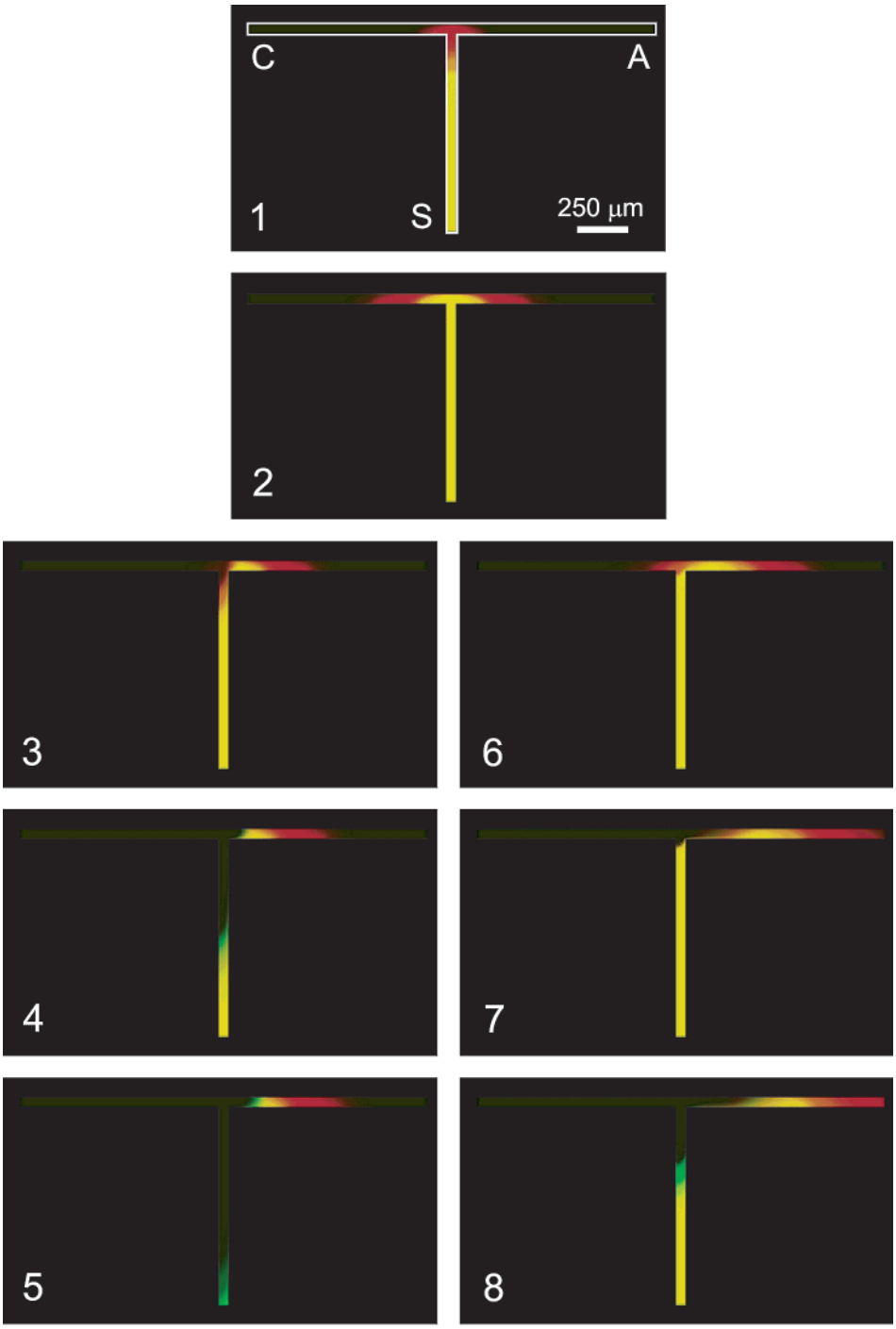

Figure 6. Finite element simulations of the direct injection process. A 100-bp fragment (red) and 1000-bp fragment (green) are simulated and the results superimposed (overlap shown in yellow). Injection conditions for the simulation mimic those used for the actual run and are constant through the first 1.8 s (frames 1 and 2) whereupon the potentials are shifted to back-biasing. In frames 3−5, the back-biasing is applied immediately. In frames 6−8, the back-biasing is delayed by 2 s.

preclude the use of a waste channel and reservoir. When a mixture of analytes having different electrophoretic mobilities is directly injected (as in all conventional CE), a large plug dominated by high-mobility species will be generated overlapping a smaller plug of lower mobility species. Finite element simulations of this process were performed with CoventorWare (Coventor, Cary, NC) using our experimental conditions (Figure 6). The relative fractions of high- and low-mobility fragments in the injected plug are shown. For any two unique fragment sizes, the imbalance of the injected masses will be directly proportional to the injection time and the fractional difference in electrophoretic mobilities in the chosen separation matrix. The effect of immediate or delayed back-biasing is also illustrated. If the back-biasing is applied immediately, the trailing half of the plug is eliminated. If back-biasing is appropriately delayed (2 s in this simulation), then the trailing portion of the high-mobility plug is clipped off.

The PDMA sieving matrix used here offers many advantages over alternatives, such as linear polyacrylamide (LPA) and

hydroxyethylcellulose (HEC). While the sieving performance of LPA is excellent, its zero-shear viscosity is orders of magnitude greater than similar PDMA polymer[27] making it difficult to load into a microchannel device. The hydrophilic chains of HEC suffer from the same viscosity effect and offer much lower sieving performance compared to that of PDMA, which is ideal for these fragment-sizing applications.

The performance of this 384-lane μCAE device is such that, assuming a 15-min cycle time, 12 000 lanes could be run in an 8-h shift. With this genotyping throughput, population studies with significant impact ($N = 5000$) could be completed in only 15 runs. Furthermore, enhanced throughput can be achieved easily by spectrally multiplexing the assays, as demonstrated in previous lower density microchip experiments.[14,28] For the present design, spectral multiplexing (first color for a size standard and three others for unknowns) should yield a throughput of 147 000 samples/day. This performance far surpasses the best commercially available 96-capillary instruments by over 20-fold (4× more capillaries with one-fifth the analysis time).

CONCLUSIONS

The success of this 384-lane μCAE chip introduces a powerful new tool for accelerating gene mapping, pharmacogenomic screening, forensics, and proteomics. The simple batch fabrication procedures employed here provide high-fidelity microstructuring of rigid, large-area, high-density electrophoresis devices with small features not feasible with comparable soft-lithographic or rapid-prototyping processes.[29] The 384-lane μCAE chip could also serve as the analyzer in a more complex bioanalysis system. As microfabricated sample preparative and purification components mature,[30] they can be integrated into the device design en masse. Our successful demonstration of genetic analysis on this 384-lane μCAE chip illustrates the powerful combination of microfabrication and electrophoretic analysis to produce the next generation of bioanalyzers.

(27) Albarghouthi, M.; Buchholz, B. A.; Doherty, E. A. S.; Bogdan, F. M.; Zhou, H. H.; Barron, A. E. *Electrophoresis* **2001**, *22*, 737−747.
(28) Medintz, I. L.; Berti, L.; Emrich, C. A.; Tom, J.; Scherer, J. R.; Mathies, R. A. *Clin. Chem.* **2001**, *47*, 1614−1621.
(29) Whitesides, G. M.; Ostuni, E.; Takayama, S.; Jiang, X. Y.; Ingber, D. E. *Annu. Rev. Biomed. Eng.* **2001**, *3*, 335−373.

ACKNOWLEDGMENT

We thank George Sensabaugh for providing samples, Jennifer Tom for sample preparation, Peter Simpson for valuable discussions on chip design, and the Chemistry machine shop and Physics electronics shop for technical assistance. Microchip devices were fabricated at the U.C. Berkeley Microfabrication Laboratory. This work was supported by grants from the National Institutes of Health (HG01399), and by the Director, Office of Science,Office of Biological and Environmental Research of the U.S. Department of Energy under Contract DE FG91ER61125.

Received for review April 10, 2002. Accepted July 16, 2002.

AC020236G

(30) Lagally, E. T.; Emrich, C. A.; Mathies, R. A. *Lab Chip* **2001**, *1*, 102−107.